Preprints of the 21st IFAC World Congress (Virtual)
Berlin, Germany, July 12-17, 2020

Dynamic Parameter Identification of a Novel Motion-Mode-Changing Quasi-Omnidirectional Mobile Platform

Florian Pucher * **Hubert Gattringer** * **Andreas Müller** *

* *Institute of Robotics, Johannes Kepler University Linz, Altenbergerstraße 69, 4040 Linz, Austria, (e-mail: {florian.pucher, hubert.gattringer, a.mueller}@jku.at).*

Abstract: In process automation of logistic systems autonomous mobile platforms play an important role with high demands on flexibility and maneuverability. Limited space can be a restriction for non-omnidirectional vehicles. In this paper a quasi-omnidirectional platform is considered which can switch between four different motion-modes: wheel alignment in a standstill, a car-like steered longitudinal motion, lateral motion and pure rotation. With the requirement of carrying heavy payloads, feed-forward control becomes an important part of the control concept. This paper presents an approach for parameter identification of this motion-mode-changing system. The equations of motion are formulated using a redundantly parameterized model, which is linear in inertia and friction parameters. For each motion-mode a kinematic model is used for elimination of the constraint forces. Not all parameters can be identified in every configuration.
The main idea is to use a combination of simple vehicle movements in the parameter identification process. The identified dynamic parameters are then validated using a more complex movement where all parameters are needed and a configuration which has not been used for identification. Experimental results for a prototype are shown.

Keywords: Mobile robots, identification and control methods, modeling

1. INTRODUCTION

Automated guided vehicles (AGVs) are often used in industrial applications to transport heavy loads. Space for navigation inside warehouses and factories is typically limited. Thus, omnidirectional AGVs are desirable. Different design concepts of omnidirectional wheeled mobile robots are found in Siciliano and Khatib (2016). In this paper a novel quasi-omnidirectional vehicle is considered. The concept of the vehicle was presented in Pucher et al. (2018) and is revisited in this paper. The platform can operate within four different motion-modes, which are wheel alignment at rest, a car-like steered motion, lateral motion and pure rotation. A prototype of the platform has been built. This paper focuses on the estimation of the dynamic parameters and presents experimental results.

Model-based control necessitates identification of inertia and friction parameters. For identification of the dynamic parameters the equations of motion (EoM) are typically formulated in a parameter-linear form using either the Lagrangian formalism or a Newton-Euler approach, see Gautier and Khalil (1988) and Grotjahn and Heimann (2000) respectively. The dynamic parameters of a non-holonomic vehicle were estimated in Tounsi et al. (1995), and parameter identification for omnidirectional mobile robots was done in Conceicao et al. (2009). A systematic way for identification of non-holonomic vehicles was presented in Stöger et al. (2017), where a redundantly parameterized model was used. This approach is also used in the following.

The paper is structured as follows: First the kinematic concept of the mobile platform is described and the resulting motion modes are discussed. In the next section the constraints are analyzed and proper generalized velocities are chosen for the kinematic model. Then the parameter-linear EoM are derived in a redundantly parameterized form which are valid for all four motion-modes. For each motion-mode the constraint forces are eliminated by left-multiplication of an orthogonal complement to the constraint Jacobian and a feed-forward control law is calculated. The identifiable parameters for every motion-mode are determined using a QR-decomposition.

The main contribution of this work is to use a combination of simple vehicle movements (wheel alignment at rest, straight vehicle motion and pure rotation) for parameter estimation so that the excitation trajectory occupies little space and can be executed using only odometry measurements. The identified parameters are then validated using a lane change trajectory in the car-like motion-mode where all of the identified dynamics parameters are needed.

2. DESCRIPTION OF THE PLATFORM

The principle setup of the mobile system is described in the following. A working prototype shown in Fig. 1 has been built, which is the basis for the experimental tests in section 7. It is a passively steered four wheel

drive mobile platform. The four wheels are driven by synchronous motors with planetary gears. In addition to the measurements of the motor positions via shaft encoders, the steering angles are also known.

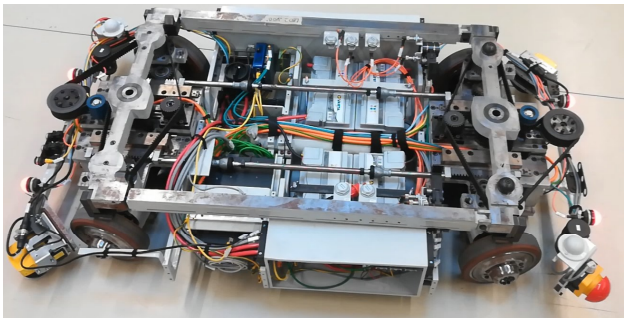

Fig. 1. Prototype of the mobile platform

2.1 Platform Kinematics

A schematic drawing of the mobile platform under consideration is shown in Fig. 2. It consists of a chassis and four driven wheels with wheel radius r. The wheels are orientable off-centered by a with the steering axes located at the corners of a rectangle. The distances between the steering axes in the longitudinal direction ${}_{ch}x$ and lateral direction ${}_{ch}y$ are l and b respectively. A mechanical coupling between steering angle of the front (index f) and rear wheel (index r) on either side of the vehicle ensures $\alpha_l = \alpha_{fl} = \alpha_{rl}$ and $\alpha_r = \alpha_{fr} = \alpha_{rr}$. Therewith, the intersection point of the two wheels at the right, respectively left, are always on a fixed line parallel to the ${}_{ch}y$-axis. From now on α_l and α_r denote the (independent) steering angles.

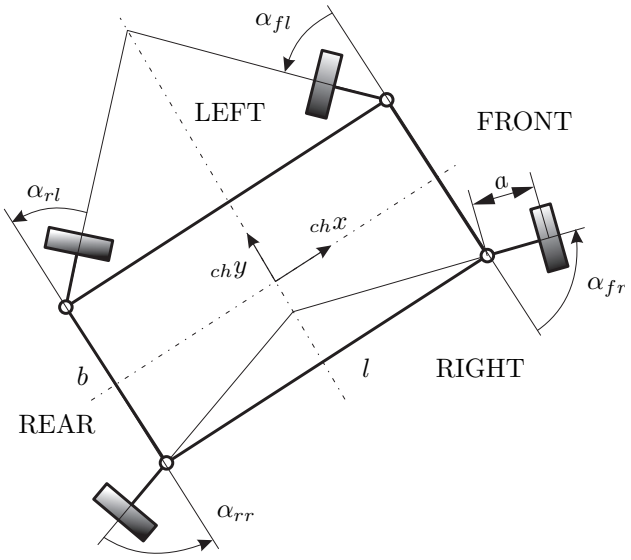

Fig. 2. Kinematic concept

2.2 Motion-Modes

The kinematics of the vehicle allows for different types of motion depending on the actual motion-mode k, depending on the steering angles, see Fig. 3. For $k = 1$ the wheel axes of the left and right vehicle side do not intersect at a common point. This is the parking mode. In this case the chassis cannot move. However, the steering angles on both sides can be adjusted independently. In the motion-mode $k = 2$ steered motion along the longitudinal chassis direction is possible. The steering angles must be controlled to hold the *instantaneous center of rotation (ICR)*.

Also lateral motion is possible as it can be seen in Fig. 3 for $k = 3$. In the current setup mechanical stops do not allow absolute values of the steering angles greater than $\pi/2$. Hence, lateral motion is not steered. Otherwise lateral motion would be analogue to mixed motion. Pure rotation of the vehicle can be achieved if the ICR is in the center of the chassis, see Fig. 3 for $k = 4$. The switching between the four different motion-modes is achieved by aligning the wheels when the platform is at rest.

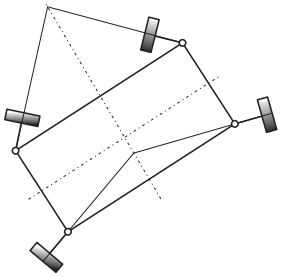

$k = 1$: Wheel alignment at rest

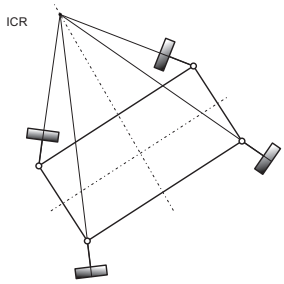

$k = 2$: Mixed motion

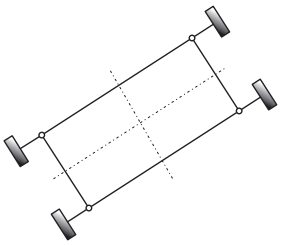

$k = 3$: Lateral motion

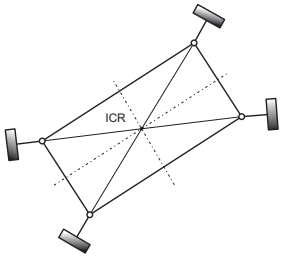

$k = 4$: Pure rotation

Fig. 3. Motion-modes $k \in \{1, 2, 3, 4\}$

3. KINEMATIC MODEL

In Fig. 4 the variables used for the description of the kinematics are shown. The minimal coordinates $\mathbf{q}^T = \left(\mathbf{q}_{ch}^T \ \boldsymbol{\alpha}^T \ \boldsymbol{\beta}^T\right)$ comprise the posture coordinates $\mathbf{q}_{ch}^T = (x \ y \ \gamma)_{ch}$, the rolling angles of the wheels $\boldsymbol{\beta}^T = (\beta_{fl} \ \beta_{rl} \ \beta_{fr} \ \beta_{rr})$ and the steering angles $\boldsymbol{\alpha}^T = (\alpha_l \ \alpha_r)$. Note that the position coordinates of the chassis x_{ch} and y_{ch} are given in the chassis fixed coordinate frame. The chassis orientation is described by γ_{ch}.

3.1 Constraints

The velocity constraints are given by pure rolling conditions, which can be written in the form

$$\begin{pmatrix} \mathbf{v}_{w,\text{lat}} \\ \mathbf{v}_{w,\text{long}} - r\dot{\boldsymbol{\beta}} \end{pmatrix} = \mathbf{A}(\boldsymbol{\alpha})\dot{\mathbf{q}} = \mathbf{0} \in \mathbb{R}^8 \tag{1}$$

where $\mathbf{v}_{w,\text{long}}$ and $\mathbf{v}_{w,\text{lat}}$ are the longitudinal and lateral wheel velocities respectively. The matrix $\mathbf{A}(\boldsymbol{\alpha})$ has the form

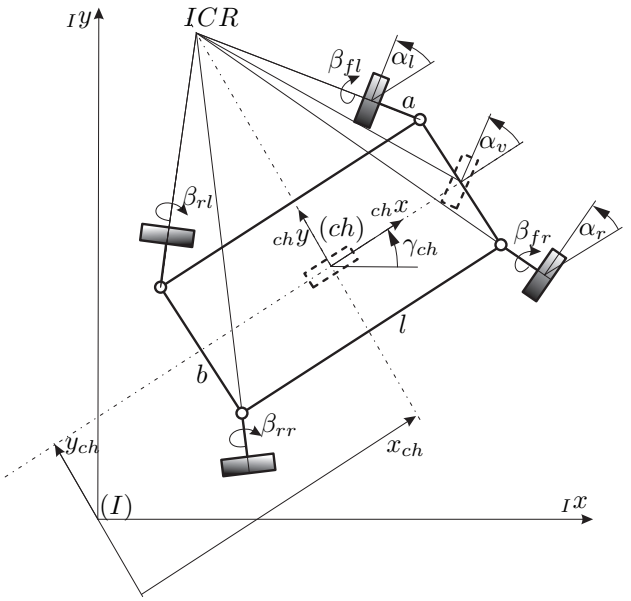

Fig. 4. Vehicle kinematics

$$\mathbf{A}(\boldsymbol{\alpha}) = \begin{bmatrix} \mathbf{A}_{ch,1}(\boldsymbol{\alpha}) & \mathbf{0} & \mathbf{0} \\ \mathbf{A}_{ch,2}(\boldsymbol{\alpha}) & \mathbf{A}_{\alpha,2} & \mathbf{A}_{\beta,2} \end{bmatrix} = [\mathbf{A}_{ch}(\boldsymbol{\alpha}) \ \mathbf{A}_{\alpha} \ \mathbf{A}_{\beta}] \quad (2)$$

which is only depending on the steering angles. This property is beneficial for various considerations, as can be seen in the next section.

3.2 Odometry

The measurements of the steering angles $\boldsymbol{\alpha}$ and the rolling angles $\boldsymbol{\beta}$ give rise to $\dot{\boldsymbol{\alpha}}$ and $\dot{\boldsymbol{\beta}}$, respectively. Using (1) and the partitioning of $\mathbf{A}(\boldsymbol{\alpha})$ in (2) the chassis velocities $\dot{\mathbf{q}}_{ch}$ can be calculated with

$$\dot{\mathbf{q}}_{ch} = -\mathbf{A}_{ch}^{+}(\boldsymbol{\alpha}) \left(\mathbf{A}_{\alpha} \dot{\boldsymbol{\alpha}} + \mathbf{A}_{\beta} \dot{\boldsymbol{\beta}} \right) \quad (3)$$

where $\mathbf{A}_{ch}^{+} = \left(\mathbf{A}_{ch}^{T} \mathbf{A}_{ch} \right)^{-1} \mathbf{A}_{ch}^{T}$ denotes the *Moore-Penrose* pseudoinverse. The vehicle posture $\mathbf{q}_{ch}$ can be obtained be time integration of $\dot{\mathbf{q}}_{ch}$. Localization and navigation of the mobile platform, as well as path tracking is beyond the scope of this paper and needs further treatment.

3.3 Generalized Velocities

The number of linear independent constraints in (1) determines a set of generalized velocities $\dot{\mathbf{s}}_k$ depending on the actual motion-mode $k \in \{1, 2, 3, 4\}$. A kinematic model in the form

$$\dot{\mathbf{q}} = \mathbf{H}_k(\boldsymbol{\alpha}) \, \dot{\mathbf{s}}_k \quad (4)$$

can be obtained for each motion-mode, so that

$$\mathbf{A}(\boldsymbol{\alpha}) \, \dot{\mathbf{q}} = \mathbf{A}(\boldsymbol{\alpha}) \, \mathbf{H}_k(\boldsymbol{\alpha}) \, \dot{\mathbf{s}}_k \equiv \mathbf{0}. \quad (5)$$

In the mixed motion-mode $k = 2$ the left and right steering angles satisfy an implicit relation of the form $f_{ICR,lr}(\boldsymbol{\alpha}) = 0$. Fig. 4 shows a kinematically equivalent single-track model. A virtual fixed wheel is placed at the center of the chassis and a virtual steering wheel at the middle of the front with distance $l/2$ to the center. This single-track-model is an intuitive abstraction. Using the similarity of triangles the relationship between the steering angles is given by

$$\frac{l/2}{\tan \alpha_l} = \frac{l/2}{\tan \alpha_r} - b \qquad = \frac{l/2}{\tan \alpha_v} - b/2 \quad (6)$$

$$f_l(\alpha_l) = f_r(\alpha_l) \qquad = f_v(\alpha_v). \quad (7)$$

The real steering angles $\boldsymbol{\alpha}$ can be computed as a function of the virtual steering angle α_v with

$$\boldsymbol{\alpha} = \mathbf{f}_{ICR}(\alpha_v) = \begin{pmatrix} f_l^{-1}(f_v(\alpha_v)) \\ f_r^{-1}(f_v(\alpha_v)) \end{pmatrix}. \quad (8)$$

Finally, the current motion-mode can be determined by

$$k = \begin{cases} 1 & \text{else} \\ 2 & \text{if} \quad f_l(\alpha_l) - f_r(\alpha_l) = f_{ICR,lr}(\boldsymbol{\alpha}) = 0 \\ 3 & \text{if} \quad \boldsymbol{\alpha}^T = \pi/2 \ \begin{pmatrix} -1 & 1 \end{pmatrix} \\ 4 & \text{if} \quad \boldsymbol{\alpha}^T = \arctan(l/b) \begin{pmatrix} -1 & 1 \end{pmatrix} \end{cases} \quad (9)$$

with numbering according to Fig. 3. The generalized velocities $\dot{\mathbf{s}}_k$ are chosen as

$$\dot{\mathbf{s}}_1^T = \dot{\boldsymbol{\alpha}}^T = (\dot{\alpha}_l \ \dot{\alpha}_r) \quad (10)$$

$$\dot{\mathbf{s}}_2^T = (\dot{\alpha}_v \ \dot{x}_{ch}) \quad (11)$$

$$\dot{\mathbf{s}}_3 = \dot{y}_{ch} \quad (12)$$

$$\dot{\mathbf{s}}_4 = \dot{\gamma}_{ch} \quad (13)$$

for intuitive interpretation of the specific motion-mode. For wheel alignment at rest ($k = 1$) the generalized velocities are the steering angular velocities left and right, $\dot{\alpha}_l$, $\dot{\alpha}_r$. In the configuration for steered forward motion ($k = 2$) the chassis velocity in longitudinal direction $\dot{x}_{ch}$ and the angular velocity of the virtual steering wheel $\dot{\alpha}_v$ are the corresponding velocities. Lateral motion ($k = 3$) uses the lateral chassis velocity $\dot{y}_{ch}$ and pure rotation ($k = 4$) the angular velocity of the chassis $\dot{\gamma}_{ch}$.

4. DYNAMICS MODEL

The dynamics are modeled by using the so called projection equation presented by Bremer (2008). Since there are different generalized velocities, the modeling uses a redundantly parameterized formulation in $\dot{\mathbf{q}}$ with constraint forces. The EoM are reformulated to be linear depending on the inertia and friction parameters. Based on this formulation a reduced model in $\dot{\mathbf{s}}_k$ is derived for each motion-mode k.

The drives are modeled with a lumped inertia parameter B_w accounting for the motor, planetary gear (with gear ratio i_G) and wheel. The wheel friction model consists of a viscous and a Coulomb part, $d_{v,w}$ and $d_{c,w}$. The same parameters are assumed for all four wheels. The chassis is modeled with mass m_{ch} and inertia C_{ch}. For the steering units the inertia parameters of front and rear axis

are combined, C_l and C_r for left and right respectively. Steering friction parameters (viscous and Coulomb part again) for left and right are accordingly denoted by $d_{v,l}$, $d_{c,l}$ and $d_{v,r}$, $d_{c,r}$. The change of the masses of steering units are neglected for the process of identification (they are added to the chassis mass). This results in a constant total vehicle inertia $C_{\text{total}}(\boldsymbol{\alpha}) \approx C_{ch} + C_l + C_r = \text{const.}$ and a neglect of the gyroscopic coupling forces between $\boldsymbol{\alpha}$ and γ_{ch}. This simplification is based on the assumption $a \ll \sqrt{l^2 + b^2}/2$.

The EoM can be written in the general form

$$\mathbf{M}(\mathbf{q}, \mathbf{p})\ddot{\mathbf{q}} + \mathbf{g}(\mathbf{q}, \dot{\mathbf{q}}, \mathbf{p}) = \mathbf{B}(\mathbf{q})\mathbf{u} + \mathbf{A}^T(\boldsymbol{\alpha})\,\boldsymbol{\lambda} \tag{14}$$

with the inertia matrix $\mathbf{M}(\mathbf{q}, \mathbf{p})$, the input matrix $\mathbf{B}(\mathbf{q})$ and the nonlinear terms $\mathbf{g}(\mathbf{q}, \dot{\mathbf{q}}, \mathbf{p})$ and constraint forces $\mathbf{A}^T(\boldsymbol{\alpha})\,\boldsymbol{\lambda}$ with the Lagrange multipliers $\boldsymbol{\lambda}$. The vector of the motor torques is $\mathbf{u} = \mathbf{M}_{\text{mot}} \in \mathbb{R}^4$. In this formulation only the rank of the matrix $\mathbf{A}^T(\boldsymbol{\alpha})$ depends on the motion-mode.

For identification of the dynamic parameters $\mathbf{p}$ a reformulation of the left hand side of (14) is required. The EoM are rewritten in the form

$$\boldsymbol{\Theta}(\mathbf{q}, \dot{\mathbf{q}}, \ddot{\mathbf{q}})\mathbf{p} = \mathbf{B}(\mathbf{q})\mathbf{u} + \mathbf{A}^T(\boldsymbol{\alpha})\,\boldsymbol{\lambda} \tag{15}$$

with the matrix $\boldsymbol{\Theta}(\mathbf{q}, \dot{\mathbf{q}}, \ddot{\mathbf{q}})$, where the left hand side is linear in the inertia and friction parameters. The EoM in the parameter form (15) can be derived systematically, see Neubauer et al. (2015). The EoM are expressed explicitly as

$$\boldsymbol{\Theta}(\mathbf{q}, \dot{\mathbf{q}}, \ddot{\mathbf{q}})\mathbf{p} = \begin{pmatrix} m_{ch}\,\ddot{x}_{ch} - m_{ch}\,\dot{y}_{ch}\dot{\gamma}_{ch} \\ m_{ch}\,\ddot{y}_{ch} + m_{ch}\,\dot{x}_{ch}\dot{\gamma}_{ch} \\ (C_{ch} + C_l + C_r)\,\ddot{\gamma}_{ch} \\ C_l\ddot{\alpha}_l + d_{v,l}\dot{\alpha}_l + d_{c,l}\tanh(\dot{\alpha}_l/\varepsilon) \\ C_r\ddot{\alpha}_r + d_{v,r}\dot{\alpha}_r + d_{c,r}\tanh(\dot{\alpha}_r/\varepsilon) \\ B_w\ddot{\boldsymbol{\beta}} + d_{v,w}\dot{\boldsymbol{\beta}} + d_{c,w}\tanh\left(\dot{\boldsymbol{\beta}}/\varepsilon\right) \end{pmatrix} \tag{16}$$

$$\mathbf{B}(\mathbf{q})\mathbf{u} = \begin{pmatrix} \mathbf{0} \\ i_G\mathbf{M}_{\text{mot}} \end{pmatrix}. \tag{17}$$

This shows that the matrix $\boldsymbol{\Theta}(\mathbf{q}, \dot{\mathbf{q}}, \ddot{\mathbf{q}})$ can be calculated easily for the set of 11 dynamic parameters

$$\begin{aligned}\mathbf{p}^T = (\; & C_l \;\; d_{v,l} \;\; d_{c,l} \;\; C_r \;\; d_{v,r} \;\; d_{c,r} \;\; \dots \\ & \dots \;\; m_{ch} \;\; C_{ch} \;\; d_{v,w} \;\; d_{c,w} \;\; B_w \;\;)^{\cdot}\end{aligned} \tag{18}$$

The tanh-function with a fixed parameter ε in (17) models Coulomb friction.

The Lagrange multipliers $\boldsymbol{\lambda}$ are eliminated by left multiplication of (15) with $\mathbf{H}_k^T(\boldsymbol{\alpha})$, which yields

$$\mathbf{H}_k^T(\boldsymbol{\alpha})\boldsymbol{\Theta}(\mathbf{q}, \dot{\mathbf{q}}, \ddot{\mathbf{q}})\mathbf{p} = \mathbf{H}_k^T(\boldsymbol{\alpha})\mathbf{B}(\mathbf{q})\mathbf{u} \tag{19}$$

where the constraint forces vanish due to (5). For each motion-mode k equation (19) can be calculated. It is the basic equation used for identification of the dynamic parameters $\mathbf{p}$ and the feed-forward control. It is important that $\mathbf{H}_k$ only depends on $\boldsymbol{\alpha}$.

5. FEED-FORWARD CONTROL

Inserting (4) and its derivative for motion-mode k

$$\ddot{\mathbf{q}} = \dot{\mathbf{H}}_k(\boldsymbol{\alpha}, \dot{\boldsymbol{\alpha}})\,\dot{\mathbf{s}}_k + \mathbf{H}_k(\boldsymbol{\alpha})\,\ddot{\mathbf{s}}_k \tag{20}$$

gives rise to the feed-forward control law

$$\mathbf{u}(\mathbf{q}, \dot{\mathbf{s}}_k, \ddot{\mathbf{s}}_k, \mathbf{p}) = \left[\mathbf{H}_k^T(\boldsymbol{\alpha})\mathbf{B}(\mathbf{q})\right]^+ \mathbf{H}_k^T(\boldsymbol{\alpha})\boldsymbol{\Theta}(\mathbf{q}, \dot{\mathbf{q}}, \ddot{\mathbf{q}})\mathbf{p} \tag{21}$$

using desired values for $\mathbf{q}$, $\dot{\mathbf{s}}_k$, and $\ddot{\mathbf{s}}_k$. The generalized torques are distributed to the motor torques using a pseudoinverse (a right inverse) of the matrix $\mathbf{H}_k^T(\boldsymbol{\alpha})\mathbf{B}(\mathbf{q})$. The same dynamic parameters $\mathbf{p}$ are used in all configurations. The trajectories $\mathbf{q}$ must fulfill the conditions (9) between the steering angles according to the corresponding configuration.

The feedback part utilizes a cascaded control scheme. For further details on the control strategy the reader is referred to Pucher et al. (2018).

6. PARAMETER IDENTIFICATION

Starting point for identification of the dynamic parameters $\mathbf{p}$ is (19). All four vehicle configurations can be used in the identification process. Furthermore, a special case of configuration 2 is considered: straight motion ($k = 2,\ \alpha_v = \dot{\alpha}_v = \ddot{\alpha}_v = 0$). Next, it is of interest which parameters can be identified for a given set of configurations.

6.1 Identifiability

Evaluating (19) for N measurements at time values t_j for $j \in \{1, \dots, N\}$ yields the overdetermined equation system

$$\underbrace{\begin{bmatrix} \mathbf{H}_k^T(\boldsymbol{\alpha})\boldsymbol{\Theta}(\mathbf{q}, \dot{\mathbf{q}}, \ddot{\mathbf{q}})|_{t=t_1} \\ \vdots \\ \mathbf{H}_k^T(\boldsymbol{\alpha})\boldsymbol{\Theta}(\mathbf{q}, \dot{\mathbf{q}}, \ddot{\mathbf{q}})|_{t=t_N} \end{bmatrix}}_{\hat{\boldsymbol{\Theta}}} \mathbf{p} = \underbrace{\begin{bmatrix} \mathbf{H}_k^T(\boldsymbol{\alpha})\mathbf{B}(\mathbf{q})\mathbf{u}|_{t=t_1} \\ \vdots \\ \mathbf{H}_k^T(\boldsymbol{\alpha})\mathbf{B}(\mathbf{q})\mathbf{u}|_{t=t_N} \end{bmatrix}}_{\hat{\boldsymbol{\tau}}} \tag{22}$$

with regressor matrix $\hat{\boldsymbol{\Theta}}$ and right hand side vector $\hat{\boldsymbol{\tau}}$. A numerical approach using a QR-decomposition $\hat{\boldsymbol{\Theta}} = \mathbf{QR}$ as presented in Gautier (1991) is used for determination of the number of identifiable parameters, called base parameters. To this end, the matrix $\hat{\boldsymbol{\Theta}}$ is filled with random values for $\dot{\mathbf{s}}_k$. In motion-mode 2 random values are used for α_v and $\boldsymbol{\alpha}$ is calculated with (8). For $k = 1$ the steering angles $\boldsymbol{\alpha}$ are independent random values. Otherwise the steering angles are fixed according to the chosen configuration.

The parameters that were identified as independent by the QR-decomposition of $\hat{\boldsymbol{\Theta}}$ are shown in table 1. Only subsets of $\mathbf{p}$ are linear independent, except for motion-mode $k = 2$ where all parameters $\mathbf{p}$ can be identified. Table 1 also shows that lateral motion and straight motion lead to the same identifiable parameters. An interesting result is that

by a combination of the steering, straight and rotation configurations all parameters are independent, except the inertia parameter B_w.

6.2 Practical Considerations

Using the mixed motion-mode for identification of the dynamic parameters has a few disadvantages. First of all, trajectory planning of the vehicle is an important aspect. If localization is based only on odometry, a large space is required for the identification process because of odometry errors. Also, a trajectory for mixed motion in general cannot be applied in all environments. Furthermore, the constraints (1) must be fulfilled. This is achieved by a proportional controller for the steering angles $\boldsymbol{\alpha}$. The control structure of the vehicle is shown in Pucher et al. (2018). If the constraints are violated, i.e. wheels are slipping, the identification result is erroneous. Another aspect is the high value of the motor torques, which are required to overcome stiction. Therefore it is easier to use motions where the steering angles remain constant. The idea is to use only basic vehicle movements for parameter estimation to increase the robustness of the identification process. The parameters then are validated with a more complex trajectory.

From now on, for the parameter identification, the combination of modes $k = 1, 2$ (with $\alpha_v \equiv 0$) and 4 is used. Excitation trajectories are represented as Fourier series for the steering angles $\boldsymbol{\alpha}$, longitudinal chassis position x_{ch}, and vehicle orientation γ_{ch}. The identification process should be applicable solely with odometry measurements. Hence, deviations from the planned vehicle orientation are unavoidable and must be considered. Therefore, the execution order of the identification trajectories is chosen to

(1) Steering of the left wheel set
(2) Steering of the right wheel set
(3) Straight motion
(4) Pure rotation

where straight motion is before pure rotation. This ensures that the direction of the straight motion is known. The space occupied by the vehicle during the identification process can be approximated by a rectangle with length $l + 2\max|x_{ch}(t)|$ and width $\sqrt{l^2 + b^2} + 2a$.

Steering left and right is split in to two separate trajectories where only one side is steering and the other side has a constant zero steering angle. This is done in order to reduce the coupling effect between both sides due to reaction forces acting on the chassis.

Table 1. Linear independent parameters

Motion-modes	Linear independent parameters
1	$C_l\ d_{v,l}\ d_{c,l}\ C_r\ d_{v,r}\ d_{c,r}$
2	$\mathbf{p}$
3	$m_{ch}\ d_{v,w}\ d_{c,w}$
4	$C_{ch}\ d_{v,w}\ d_{c,w}$
2 ($\alpha_v \equiv 0$)	$m_{ch}\ d_{v,w}\ d_{c,w}$
1, 2 ($\alpha_v \equiv 0$), 4	$C_l\ d_{v,l}\ d_{c,l}\ C_r\ d_{v,r}\ d_{c,r}\ m_{ch}\ C_{ch}\ d_{v,w}\ d_{c,w}$

6.3 Regularization

By splitting $\mathbf{p}^T = \begin{pmatrix}\mathbf{p}_1^T & \mathbf{p}_2^T\end{pmatrix}$ into independent parameters $\mathbf{p}_1^T = (C_l\ d_{v,l}\ d_{c,l}\ C_r\ d_{v,r}\ d_{c,r}\ m_{ch}\ C_{ch}\ d_{v,w}\ d_{c,w})$ and dependent parameters $\mathbf{p}_2 = B_w$ equation (22) becomes

$$\begin{bmatrix}\hat{\boldsymbol{\Theta}}_1 & \hat{\boldsymbol{\Theta}}_2\end{bmatrix}\begin{pmatrix}\mathbf{p}_1\\ \mathbf{p}_2\end{pmatrix} = \hat{\boldsymbol{\tau}} \tag{23}$$

with columns $\hat{\boldsymbol{\Theta}}_1$ and $\hat{\boldsymbol{\Theta}}_2$ of $\hat{\boldsymbol{\Theta}}$ corresponding to $\mathbf{p}_1$ and $\mathbf{p}_2$, respectively. The linear dependent columns can be written as a linear combination of the independent coumns, i.e. $\hat{\boldsymbol{\Theta}}_2 = \hat{\boldsymbol{\Theta}}_1\boldsymbol{\kappa}$ with an appropriate matrix $\boldsymbol{\kappa}$. Hence, a set of base parameters $\mathbf{p}_B = \mathbf{p}_1 + \boldsymbol{\kappa}\mathbf{p}_2$ can be determined with $\hat{\boldsymbol{\Theta}}_1\mathbf{p}_B = \hat{\boldsymbol{\tau}}$. However, the base parameters cannot be used for feed-forward control in motion-mode 2. Therefore, it is assumed that an estimate of the inertia B_w is available from data-sheets or from a single axis parameter identification without ground contact. With knowledge of the dependent parameters $\mathbf{p}_2$ equation (23) can be written as

$$\hat{\boldsymbol{\Theta}}_1\mathbf{p}_1 = \hat{\boldsymbol{\tau}} - \hat{\boldsymbol{\Theta}}_2\mathbf{p}_2 \tag{24}$$

where only $\mathbf{p}_1$ has to be identified. A scaling of the parameters with a weighting matrix $\mathbf{W}$, as proposed in Lawson and Hanson (1995) is used for a better conditioning of the least-squares problem (24), which becomes

$$\underbrace{\hat{\boldsymbol{\Theta}}_1\mathbf{W}}_{\hat{\boldsymbol{\Theta}}_{1,w}}\underbrace{\mathbf{W}^{-1}\mathbf{p}_1}_{\mathbf{p}_{1,w}} = \hat{\boldsymbol{\tau}} - \hat{\boldsymbol{\Theta}}_2\mathbf{p}_2. \tag{25}$$

The weighting matrix $\mathbf{W}$ is a diagonal matrix which contains the Euclidean norm $\|\hat{\boldsymbol{\theta}}_{1,i}\|_2$ of the columns of $\hat{\boldsymbol{\Theta}}_1$. The solution of (25) is $\mathbf{p}_1 = \mathbf{W}\mathbf{p}_{1,w} = \mathbf{W}\hat{\boldsymbol{\Theta}}_{1,w}^{+}(\hat{\boldsymbol{\tau}} - \hat{\boldsymbol{\Theta}}_2\mathbf{p}_2)$.

7. EXPERIMENTAL RESULTS

Table 2. Identified Parameters

Name	Value	Std. Deviation	Unit
C_l	0.3342	0.0685	kg·m^2
$d_{v,l}$	4.4649	0.6807	Nm·s/rad
$d_{c,l}$	12.9458	0.7664	Nm
C_r	0.4501	0.0641	kg·m^2
$d_{v,r}$	2.4820	0.6864	Nm·s/rad
$d_{c,r}$	17.1071	0.8061	Nm
m_{ch}	842.0684	0.9934	kg
C_{ch}	286.5955	1.1835	kg·m^2
$d_{v,w}$	0.7316	0.0062	Nm·s/rad
$d_{c,w}$	3.9656	0.0125	Nm

The value $B_w = 0.121$ kg·m^2 for the combined motor-gear-wheel inertia was estimated by single-axis identification without ground contact. All zero-phase filters, including those for first and second order time derivatives, use a cutoff frequency of $\omega_g = 40$ rad/s. The parameter used in the tanh-function is set to $\varepsilon = 0.01$ rad/s. Stiction effects are respected by setting a row of the equation system to zero if the corresponding generalized velocity is below a threshold. Measurement data is sampled with

$T_s = 2$ ms. Table 2 shows the values of the identified dynamic parameters $\mathbf{p}_1$ and their standard deviations. The value of the condition number is $\text{cond}(\hat{\mathbf{\Theta}}_1^T \hat{\mathbf{\Theta}}_1) = 11.56$.

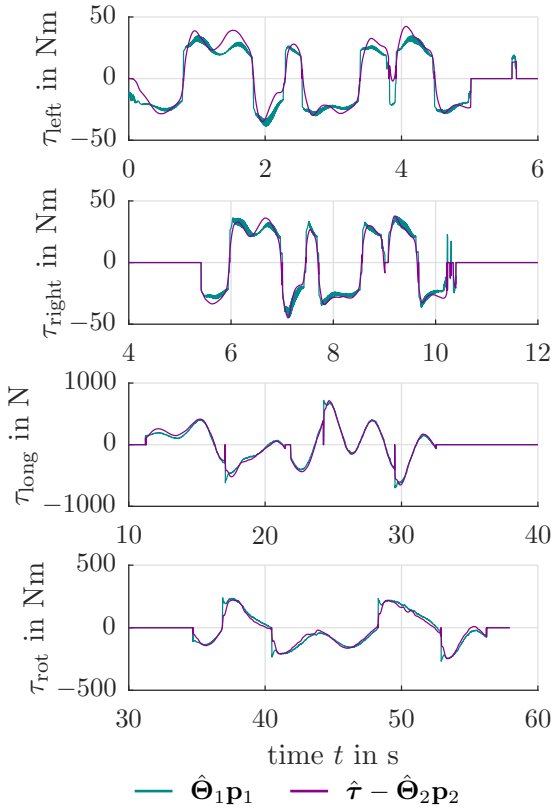

Fig. 5. Identification experiment: generalized torques

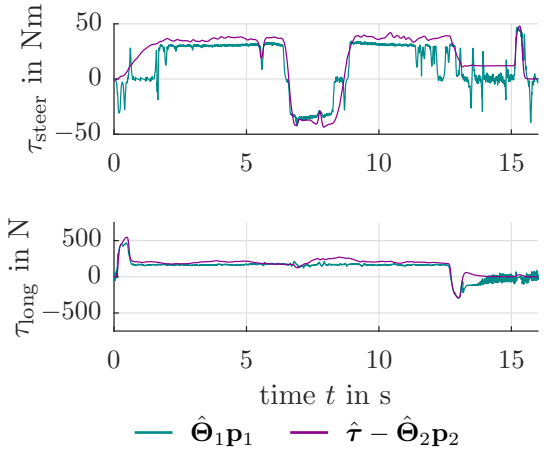

Fig. 6. Validation experiment: generalized torques

For evaluation of the identified model parameters the generalized torques on the left hand side $\hat{\mathbf{\Theta}}_1\mathbf{p}_1$ and right hand side $\hat{\boldsymbol{\tau}} - \hat{\mathbf{\Theta}}_2\mathbf{p}_2$ of (24) are compared. The generalized torques resulting from measurements of the identification process are shown in Fig. 5. Note that the configurations succeed each other, hence different time windows are shown. For validation, a lane change was planned using the mixed motion configuration $k = 2$. Fig. 6 shows the comparison of the corresponding generalized torques for the validation trajectory. Stiction effects were not eliminated in this figure. Hence, there are bigger differences, especially in the steering torques. The comparison of the torques in Fig. 5 and Fig. 6 shows that the identified dynamic parameters can be also used in the mixed motion configuration. For the identification and validation experiments see `https://youtu.be/q2gh6s6vKCA`.

8. CONCLUSION

In this paper the dynamic parameters of a pseudo-omnidirectional mobile robot with four different motion-modes were identified. The EoM were formulated using a redundantly parameterized model linear in inertia and friction parameters. These are applicable in all motion-modes. A combination of three configurations with simple movements was used for parameter identification. Experimental results are reported for a real prototype. Validation was done with a more complex motion in a configuration, which was not used in the previous identification process.

ACKNOWLEDGEMENTS

This work has been supported by the “LCM – K2 Center for Symbiotic Mechatronics” within the framework of the Austrian COMET-K2 program.

REFERENCES

Bremer, H. (2008). *Elastic multibody dynamics*. Springer.

Conceicao, A.S., Moreira, A.P., and Costa, P.J. (2009). Practical approach of modeling and parameters estimation for omnidirectional mobile robots. *IEEE/ASME transactions on mechatronics*, 14(3), 377–381.

Gautier, M. (1991). Numerical calculation of the base inertial parameters of robots. *Journal of robotic systems*, 8(4), 485–506.

Gautier, M. and Khalil, W. (1988). On the identification of the inertial parameters of robots. In *Proceedings of the 27th IEEE Conference on Decision and Control*, 2264–2269. IEEE.

Grotjahn, M. and Heimann, B. (2000). Determination of dynamic parameters of robots by base sensor measurements. *IFAC Proceedings Volumes*, 33(27), 279–284.

Lawson, C.L. and Hanson, R.J. (1995). *Solving least squares problems*, volume 15. Siam.

Neubauer, M., Gattringer, H., and Bremer, H. (2015). A persistent method for parameter identification of a seven-axes manipulator. *Robotica*, 33(5), 1099–1112.

Pucher, F., Gattringer, H., Stöger, C., Müller, A., and Single, U. (2018). Modeling and analysis of a novel passively steered 4wd mobile platform concept. In *International Conference on Robotics in Alpe-Adria Danube Region*, 264–271. Springer.

Siciliano, B. and Khatib, O. (2016). *Springer handbook of robotics*. Springer.

Stöger, C., Gattringer, H., and Müller, A. (2017). Parameter identification of non-holonomic omnidirectional vehicles using a redundantly parameterized model. *PAMM*, 17(1), 171–172.

Tounsi, M., Lebret, G., and Gautier, M. (1995). Dynamic control of a nonholonomic mobile robot in cartesian space. In *Proceedings of 1995 34th IEEE Conference on Decision and Control*, volume 4, 3825–3830. IEEE.